Ru(II) with chelating containing N$_4$-type donor quadridentate Pd-oxime metal complexes: Syntheses, spectral characterization, thermal and catalytic properties

Ahmet Kilic [a,*], Feyyaz Durap [b], Murat Aydemir [b], Akin Baysal [b], Esref Tas [a]

[a] Department of Chemistry, University of Harran, 63190 Sanliurfa, Turkey
[b] Department of Chemistry, University of Dicle, 21280 Diyarbakir, Turkey

ABSTRACT

Five new metal complexes [Pd(LH)$_2$] (**1**), [Pd(L)$_2$Ru$_2$(bpy)$_4$](ClO$_4$)$_2$ (**2**), [Pd(L)$_2$Ru$_2$(phen)$_4$](ClO$_4$)$_2$ (**3**), [Pd(L)$_2$Ru$_2$(dafo)$_4$](ClO$_4$)$_2$ (**4**) and [Pd(L)$_2$Ru$_2$(dcbpy)$_4$](ClO$_4$)$_2$ (**5**), (where, L = ligand, bpy = 2,2′-bipyridine, phen = 1,10-phenantroline, dafo = 4,5-diazafluoren-9-one and dcbpy = 3,3′-dicarboxy-2,2′-bipyridine) have been isolated and characterized by UV–VIS, FT-IR, ^{1}H NMR, magnetic susceptibility measurements, elemental analysis, molar conductivity, X-ray powder techniques, thermal analyses and their morphology studied by SEM measurements. IR spectra show that the ligand acts in a tetradentate manner and coordinates N$_4$ donor groups of LH$_2$ to Pd^{II} ion. The disapperance of H-bonding (O–H···O) in the trinuclear Ru^{II}–Pd^{II}–Ru^{II} metal complexes, the Ru^{II} ion centered into the main oxime core by the coordination of the imino groups while the two Ru^{II} ions coordinate dianionic oxygen donors of the oxime groups and linked to the ligands of bpy, phen, dafo and dbpy. The X-powder results show that **1** metal complex is indicating crystalline nature, not amorphous nature. Whereas, the X-ray powder pattern of the ligand (LH$_2$) with **2**, **3**, **4** and **5** exhibited only broad humps, indicating its amorphous nature. The catalytic activity of three different complexes were tested in the Suzuki coupling reaction. The **1**, **4** and **5** metal complexes catalyse Suzuki coupling reaction between phenylboronic acid and arylbromides affording biphenyls. Also, the thermal results shown that the most stable complex is **1** compound while the less stable is **4** compound.

© 2008 Elsevier B.V. All rights reserved.

1. Introduction

Considerable attention has focused on the preparation and properties of ruthenium(II) heterocyclic ligand complexes due to their stability and photophysical properties. Such metal complexes ranging from simple monometallic to larger arrays have been reviewed by a number of contributors in the area [1]. Also, there is continuing interest in the chemistry of ruthenium(II) polypyridyl metal complexes because of their possible use in photochemical storage of energy or as redox catalysts [2], molecular wires [3], biosensor [4], therapeutic agent applications [5], materials for molecular electronics and photonics [6] and electroluminescent display devices [7]. Metal-to-ligand charge transfer (MCLT) transitions dominate photophysical and redox behaviour such complexes. The metal-to-ligand charge transfer absorption can be extended to longer wavelengths by appropriate substituent changes on chromophoric ligands [8]. The nature of the ligands around the metal has been found to dramatically affect the energy conversion process. Particulary, the introduction of electronic effects via electron-donor substituents on 2,2′-bipyridine (bpy) 1,10-phenanthro-

line (phen), 4,5-diazafluoren-9-one (dafo) and 3,3′-dicarboxy-2,2′-bipyridine (dcbpy) ligands notably improved the absorption in the visible region for efficient sunlight collection [9]. While (oxime)ruthenium complexes are still relativity rare, we have selected the *cis*-bis(-bpy)ruthenium(II), *cis*-bis(-phen)ruthenium(II), *cis*-bis(-dafo)ruthenium(II) and *cis*-bis(-dcbpy)ruthenium(II) moiety as a platform for studies utilizing the symmetric *vic*-dioxime: *N*-(4-amino-1-benzyl piperidine)-phenylglyoxime [10]. These complexes have enabled us to systematically probe the phenomenon of proton-coupled electron transfer that occurs when oxime ligand is coordinated to a redox active metal center [11].

In this study, we have prepared mononuclear Pd^{II} and trinuclear Ru^{II}–Pd^{II}–Ru^{II} type-metal complexes. Synthesis, characterization, spectroscopic, and catalytic activities of the new *vic*-dioxime metal complexes have been investigated. The metal complexes have been identified by a combination of ^{1}H NMR spectra, FT-IR spectra, UV–VIS spectra, magnetic susceptibility measurements, X-ray powder diffraction measurements, elemental analysis, molar conductivity measurements and their morphology studied by SEM. The first aim of this study is to prepare and characterized a new different mononuclear and trinuclear metal complexes. The second aim is to understand catalytic activity of the coordination of different groups such as H-bond (O−H···O), 4,5-diazafluoren-9-one (dafo) and

* Corresponding author.
E-mail address: kilica63@harran.edu.tr (A. Kilic).

3,3′-dicarboxy-2,2′-bipyridine (dcbpy) to the oxime moieties through two oxygen donor atoms. Third aim is to understand their crystalline or amorphous structures by X-ray powder analysis as well. Fourth aim is to understand their thermal properties by thermal gravimetric analyses (TGA) and differential thermal analyses (DTA) as well.

2. Experimental

All reagents and solvents were of reagent-grade quality and obtained from commercial suppliers (Fluka). Tetra-*n*-butylammonium perchlorate (TBAP, Fluka) was used as received. Elemental analysis was carried out on a LECO CHNS model 932 elemental analyzer. FT-IR spectra were recorded on a Perkin–Elmer Spectrum RXI FT-IR Spectrometer as KBr pellets. ^{1}H NMR spectra were recorded on a Bruker-Avence 400 MHz spectrometers. Magnetic susceptibilities were determined on a Sherwood Scientific Magnetic Susceptibility Balance (Model MK1) at room temperature (25 °C) using Hg[Co(SCN)$_4$] as a calibrant; diamagnetic corrections were calculated from Pascal's constants [12,13]. UV–VIS spectra were recorded on a Perkin–Elmer Lambda 25 PC UV–VIS spectrometer. Molar conductivities (Λ_M) were recorded on a Inolab Terminal 740 WTW Series. X-ray powder was recorded on a Rigaku Ultima III Series. The thermal analyses measurements (TGA and DTA) were carried out on a Setaram Labsys TG-16 thermobalance under a nitrogen atmosphere. The scanning electron microscopy (SEM) measurements were carried out on a Zeiss Evo 50 Series. The samples were sputter coated with carbon by Balzers Med 010 to prevent charging when analyzed by the electron beam. GC analyses were performed on a HP 6890N Gas Chromatograph equipped with capillary column (5% biphenyl, 95% dimethylsiloxane) (30 m × 0.32 mm × 0.25 μm). Ligand (LH$_2$) (Fig. 1) [14], cis-[Ru(bpy)$_2$Cl$_2$] · 2H$_2$O cis-[Ru(phen)$_2$Cl$_2$] · 2H$_2$O, cis-[Ru(dafo)$_2$Cl$_2$] · 2H$_2$O and cis-[Ru(dcbpy)$_2$Cl$_2$] · 2H$_2$O [15], 4,5-diazafluoren-9-one (dafo) [16], 3,3′-dicarboxy-2,2′-bipyridine (dcbpy) [17] were prepared according to the literature procedures.

2.2. Synthesis of the [Pd(LH)$_2$] metal complex 1

A solution of palladium(II) acetate (0.28 g, 1.22 mmol) in absolute ethanol (25 cm^3) was added to a solution of ligand (LH$_2$) (0.86 g, 2.44 mmol), in absolute ethanol (60 cm^3) at 55–60 °C. A distinct change was observed in color from colorless to pale brown under a N$_2$ atmosphere with continuous stirring. Then, a decrease in the pH of the solution was observed. The pH of the solution was *ca.* 1.5–3.0 and was adjusted to 4.5–5.5 by the addition of a 1% triethylamine solution in EtOH. After heating the mixture for 5 h in a water bath, the precipitate was filtered off, washed with H$_2$O and diethyl ether several times, and dried in vacuo at 35 °C. Yield: (78%), color: pale brown, m.p. = 204 °C. Anal. Calc. for C$_{40}$H$_{46}$N$_8$O$_4$Pd (MW: 808.5 g/mol): C, 59.37; H, 5.69; N, 13.85. Found: C, 59.26; H, 5.56; N, 13.71%. Λ_M = 33 Ω^{-1}cm^2 mol^{-1}, μ_{eff} = Dia, IR (KBr pellets, υ_{max}/cm^{-1}): 3392 υ(NH), 3060–3019 υ(Ar–H), 2949–2752 υ(Aliph-H), 1692 υ(O–H···O), 1597 υ(C=N), 1334 and 976 υ(N–O), 459 υ(Pd–N). UV–VIS (λ_{max}, nm, * = shoulder peak): 274, 326, 351, 432* (in Acetone) and 266, 311, 434 (in DMF). ^{1}H NMR (DMSO-d_6, TMS, δ ppm) δ: 15.28 (s, 2H, O–H···O), 4.35 (s, 2H, NH), 7.48–7.23 (m, 20H, Ar-CH), 3.61 (s, 2H, N-CH), 2.62 (s, 4H, N-CH$_2$), 2.38 (s, 4H, N-CH$_2$), 1.92 (s, 4H, Cyc-CH$_2$) and 1.24–1.06 (m, 4H, Cyc-CH$_2$).

2.3. Synthesis of the [Pd(L)$_2$Ru$_2$(X)$_4$](ClO$_4$)$_2$ metal complexes

In this study, the complexes [Pd(L)$_2$Ru$_2$(bpy)$_4$](ClO$_4$)$_2$ (2), [Pd(L)$_2$Ru$_2$(phen)$_4$](ClO$_4$)$_2$ (3), [Pd(L)$_2$Ru$_2$(dafo)$_4$](ClO$_4$)$_2$ (4) and [Pd(L)$_2$Ru$_2$(dcbpy)$_4$](ClO$_4$)$_2$ 5 (where, L = ligand, bpy = 2,2′-bipyri-dine, phen = 1,10-phenantroline, dafo = 4,5-diazafluoren-9-one and dcbpy = 3,3′-dicarboxy-2,2′-bipyridine) were synthesized. [RuCl$_2$(bpy)$_2$] · 2H$_2$O (0.2 g, 0.38 mmol), [RuCl$_2$(phen)$_2$] · 2H$_2$O (0.2 g, 0.34 mmol), [RuCl$_2$(dafo)$_2$] · 2H$_2$O (0.2 g, 0.34 mmol) and [RuCl$_2$(dcbpy)$_2$] · 2H$_2$O (0.2 g, 0.28 mmol) were refluxed in ethanol–water–DMF mixture (40 ml/10 ml/2 ml) for 45 min. The complex [Pd(LH)$_2$] (0. 15 g, 0.19 mmol for 2, 0.14 g, 0.17 mmol for 3, 0.14 g, 0.17 mmol for 4 and 0.11 g, 0.14 mmol for 5) were then added and heating were maintained for 36 h. When the solutions finally turned red-brown, it was cooled to room temperature and equal volume of saturated aqueous NaClO$_4$ solutions were added under vigorous stirring. Then, the final products washed three times with water (10 ml) and diethyl ether (10 ml). The products were recrystallized from a mixture of CHCl$_3$–EtOH.

[Pd(L)$_2$Ru$_2$(bpy)$_4$](ClO$_4$)$_2$ (2): Yield: (64%), color: red, m.p. = 153 °C. Anal. Calc. for C$_{80}$H$_{76}$Cl$_2$N$_{16}$O$_{12}$PdRu$_2$ (MW: 1833 g/mol): C, 52.42; H, 4.18; N, 12.23. Found: C, 52.18; H, 3.98; N, 12.54%. Λ_M = 201 Ω^{-1}cm^2 mol^{-1}, μ_{eff} = Dia, IR (KBr pellets, υ_{max}/cm^{-1}): 3398 υ(NH), 3090–3031 υ(Ar-H), 2924–2853 υ(Aliph-H), 1604 υ(C=N), 1358 and 979 υ(N–O), 1071 and 624 υ(ClO$_4$) and 520 υ(Ru–N). UV–VIS (λ_{max}, nm, * = shoulder peak): 310, 316, 420, 460*, 567 (in Acetone) and 268, 294, 317, 380*, 450, 541* (in DMF). ^{1}H NMR (DMSO-d_6, TMS, δ ppm): 8.37 (d, 8H, J = 16, Ar-CH$'_{a,a}$), 8.60 (d, J = 8, 8H, Ar-CH$'_{b,b}$), 9.14 (d, 8H, J = 5.6, Ar-CH$'_{c,c}$), 7.84 (s, 8H, Ar-CH$'_{d,d}$), 7.82–7.80 (m, 20H, Ar-CH$_{others}$), 4.62 (s, 2H, NH), 3.18 (s, 2H, N-CH), 2.89 (s, 4H, N-CH$_2$), 2.74 (s, 8H, N-CH$_2$), 1.22–1.18 (d, J = 16, 8H, Cyc-CH$_2$).

[Pd(L)$_2$Ru$_2$(phen)$_4$](ClO$_4$)$_2$ (3): Yield: (68%), color: red–brown, m.p. = 224 °C. Anal. Calc. for C$_{88}$H$_{76}$Cl$_2$N$_{16}$O$_{12}$PdRu$_2$ (MW: 1929.1 g/mol): C, 54.79; H, 3.97; N, 11.62. Found: C, 54.47; H, 3.85; N, 11.69%. Λ_M = 198 Ω^{-1}cm^2 mol^{-1}, μ_{eff} = Dia, IR (KBr pellets, υ_{max}/cm^{-1}): 3392 υ(NH), 3061 υ(Ar-H), 2960–2853 υ(Aliph-H), 1602 υ(C=N), 1361 and 971 υ(N–O), 1088, 623 υ(ClO$_4$) and 524 υ(Ru–N). UV–VIS (λ_{max}, nm, * = shoulder peak): 293, 309, 324, 457 (in Acetone) and 270, 291*, 462 (in DMF). ^{1}H NMR (DMSO-d_6, TMS, δ ppm): 8.09 (d, 8H, J = 5.2, Ar-CH$'_{a,a}$), 8.39 (s, 8H, Ar-CH$'_{b,b}$), 8.76 (d, 8H, J = 8, Ar-CH$'_{c,c}$), 7.79 (s, 8H, Ar-CH$'_{d,d}$), 7.77–7.75 (m, 20H, Ar-CH$_{others}$), 4.55 (s, 2H, NH), 3.58 (s, 2H, N-CH), 2.12 (s, 12H, N-CH$_2$), 1.24 (s, 4H, Cyc-CH$_2$) and 1.15 (s, 4H, Cyc-CH$_2$).

[Pd(L)$_2$Ru$_2$(dafo)$_4$](ClO$_4$)$_2$ (4): Yield: (58%), color: red–brown, m.p. = 276 °C. Anal. Calc. for C$_{84}$H$_{68}$Cl$_2$N$_{16}$O$_{16}$PdRu$_2$ (MW: 1937 g/mol): C, 52.09; H, 3.54; N, 11.57. Found: C, 51.93; H, 3.61; N, 11.64%. Λ_M = 208 Ω^{-1}cm^2 mol^{-1}, μ_{eff} = Dia, IR (KBr pellets, υ_{max}/cm^{-1}): 3386 υ(NH), 3072 υ(Ar-H), 2954–2847 υ(Aliph-H), 1734 υ(C=O), 1615 υ(C=N), 1364 and 947 υ(N–O), 1077 and 624 υ(ClO$_4$) and 521 υ(Ru–N). UV–VIS (λ_{max}, nm, * = shoulder peak): 277, 302, 319, 326, 447 (in Acetone) and 271, 312, 382*, 564* (in DMF). ^{1}H NMR (DMSO-d_6, TMS, δ ppm): 7.53 (s, 8H, Ar-CH$'_{a,a}$), 8.86 (s, 8H, Ar-CH$'_{b,b}$), 8.24 (d, 8H, Ar-CH$'_{c,c}$), 7.38–7.08 (m, 20H, Ar-CH$_{others}$), 4.46 (s, 2H, NH), 3.52 (s, 2H, N-CH), 2.63 (s, 4H, N-CH$_2$), 2.31 (s, 8H, N-CH$_2$), 1.23 (s, 4H, Cyc-CH$_2$) and 1.10 (s, 4H, Cyc-CH$_2$).

[Pd(L)$_2$Ru$_2$(dcbpy)$_4$](ClO$_4$)$_2$ 5: Yield: (63%), color: red–brown, m.p. = >300 °C. Anal. Calc. for C$_{88}$H$_{76}$Cl$_2$N$_{16}$O$_{28}$PdRu$_2$ (MW: 2185.1 g/mol): C, 48.37; H, 3.51; N, 10.26. Found: C, 48.19; H, 3.46; N, 10.37%. Λ_M = 211 Ω^{-1}cm^2 mol^{-1}, μ_{eff} = Dia, IR (KBr pellets, υ_{max}/cm^{-1}): 3420 υ(OH), 3381 υ(NH), 3078 υ(Ar-H), 2954-2847 υ(Aliph-H), 1718 υ(C=O), 1616 υ(C=N), 1381 and 965 υ(N–O), 1077, 624 υ(ClO$_4$) and 526 υ(Ru–N). UV–VIS (λ_{max}, nm, * = shoulder peak): 293, 303, 308, 324 (in Acetone) and 301, 395, 597* (in DMF). ^{1}H NMR (DMSO-d_6, TMS, δ ppm): 10.10 (d, 2H, J = 8, COOH), 7.38 (s, 8H, Ar-CH$'_{a,a}$), 8.24 (s, 8H, Ar-CH$'_{b,b}$), 7.79 (s, 8H, Ar-CH$'_{c,c}$), 7.18–7.06 (m, 20H, Ar-CH$_{others}$), 4. 64 (s, 2H, NH), 4.21 (s, 2H, N-CH), 2.64 (s, 4H, N-CH$_2$), 2.28 (s, 8H, N-CH$_2$), 2.09 (s, 4H, Cyc-CH$_2$) and 1.22–1.20 (m, 4H, Cyc-CH$_2$) (see Fig. 2).

3. Results and discussion

The complex of the general formula [Pd(LH)$_2$] was synthesized by the reactions of ligand (LH$_2$) with the respective Pd(CH$_3$COO)$_2$ in a 1:2 molar ratio in ethanol and the metal complexes of the general formula [Pd(L)$_2$Ru$_2$(X)$_4$](ClO$_4$)$_2$ (where, L = ligand, X = 2,2′-bipyridine, 1,10-phenantroline, 4,5-diazafluoren-9-one, 3,3′-dicarboxy-2,2′-bipyridine) were synthesized by the reactions of [Pd(LH)$_2$] with the respective RuCl$_2$(bpy)$_2$ · 2H$_2$O, RuCl$_2$(phen)$_2$ ·

2H$_2$O, RuCl$_2$(dafo)$_2$ · 2H$_2$O or RuCl$_2$(dcbpy)$_2$ · 2H$_2$O and then added NaClO$_4$ in ethanol–water–DMF mixture, as shown in Fig. 2. For the [Pd(L)$_2$Ru$_2$(X)$_4$](ClO$_4$)$_2$ complexes, the reactions of [Pd(LH)$_2$] with the system RuCl$_2$(bpy)$_2$ · 2H$_2$O, RuCl$_2$(phen)$_2$ · 2H$_2$O, RuCl$_2$(dafo)$_2$ · 2H$_2$O or RuCl$_2$(dcbpy)$_2$ · 2H$_2$O/NaClO$_4$ was carried out (Eq. (1)) [18]

$$2[RuCl_2(X)_2 \cdot 2H_2O] + [Pd(LH)_2] + 2NaClO_4$$
$$\rightarrow [Pd(L)_2Ru_2(X)_4](ClO_4)_2 + 2NaCl + 2HCl \qquad (1)$$

X = 2,2′-bipyridine, 1,10-phenanthroline, 4,5-diazafluoren-9-one and 3,3′-dicarboxy-2,2′-bipyridine.

Magnetic susceptibility measurements provide sufficient data to characterize the structure of the metal complexes. Magnetic moments measurements of all metal complexes carried out at 25 °C. The results show that mononuclear 1 with trinuclear 2, 3, 4 and 5 metal complexes are diamagnetic. The morphology and particle size of the compounds have been illustrated by the scanning electron micrography (SEM). Fig. 4a and b depicts the SEM images of 1 and 4 metal complexes. We noted that there is a uniform matrix of the synthesized complexes in the pictograph. This leads us to believe that we are dealing with homogeneous phase material. The crystalline shape is observed in the 1 complex and the amorphous shape is observed in the 4 complex.

Fig. 1. Structure of ligand (LH$_2$).
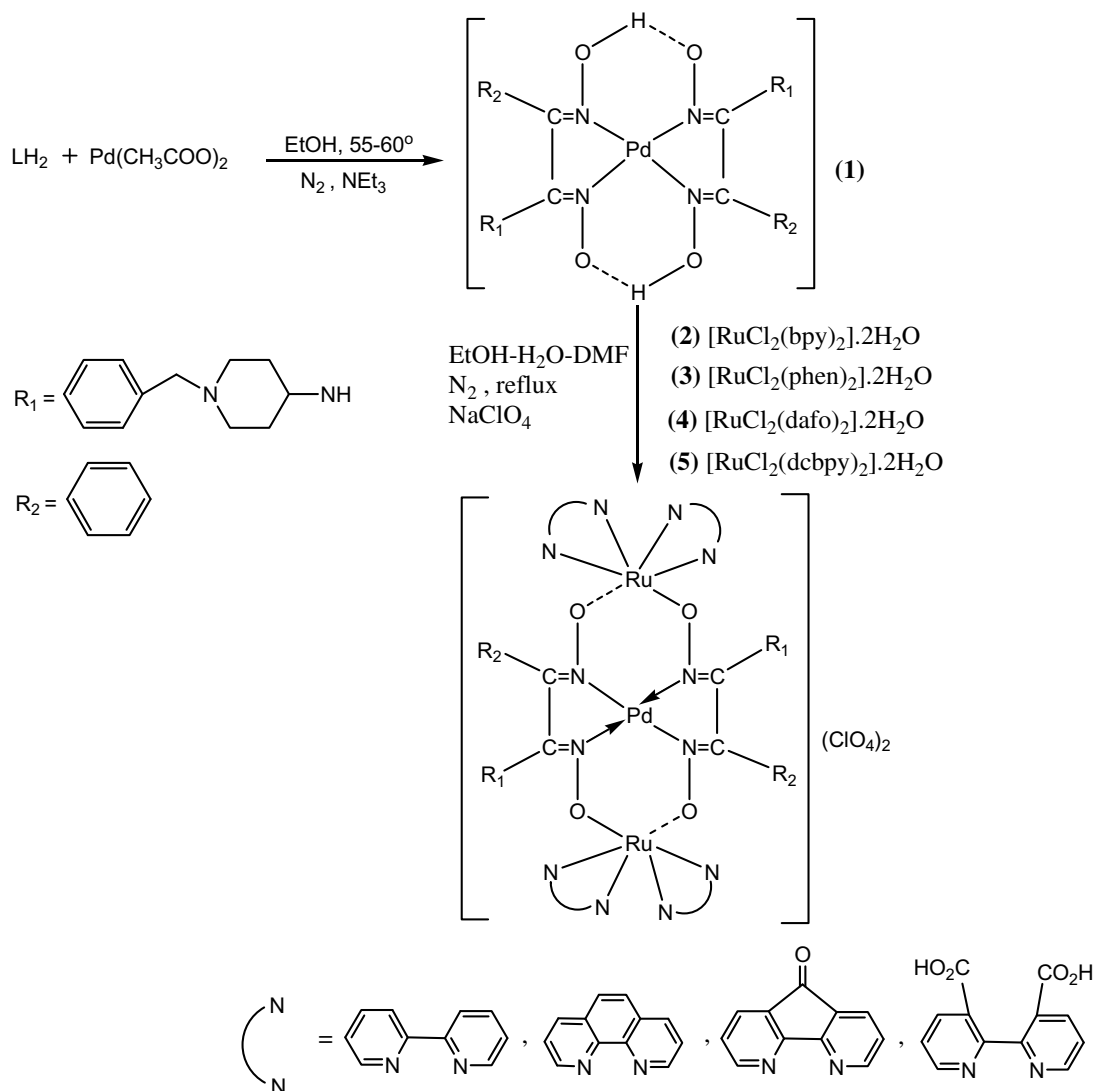
Fig. 2. The proposed structure for 2, 3, 4 and 5 metal complexes.

3.1. NMR Spectra

The data of the ^{1}H NMR spectra (in DMSO-d_6) obtained for **1**, **2**, **3**, **4** and **5** metal complexes are given in Section 2. The ^{1}H NMR spectra of the diamagnetic metal complex **1** was characterized by the existence of intra-molecular D$_2$O-exchangeable H-bridge (O−H···O) protons which were observed by a new signals at low field, δ = 15.25 ppm for **1** complex. The other protons were observed at different field than ligand [14]. In the ^{1}H NMR spectra of **2**, **3**, **4** and **5**, the D$_2$O-exchangeable hydrogen-bridged protons, which were evident in **1**, disappear after the formation of the bpy, phen, dafo or dcbpy-bridged metal complexes. In the ^{1}H NMR spectra of **2**, **3**, **4** and **5** complexes, the proton Ar-CH$_{others}$ of phenyl ring is shifted different field compared to those of the free ligand. The ^{1}H NMR spectra provide information on the *cis*-coordination of the bpy, phen, dafo and dcbpy ligands. As reported previously, each of the 2,2′-bipyridine (bpy) 1,10-phenanthroline (phen), 4,5-diazafluoren-9-one (dafo) or 3,3′-dicarboxy-2,2′-bipyridine (dcbpy) rings of a bpy, phen, dafo or dcbpy ligands are magnetically nonequivalent due to the *cis*-geometry of the complexes [12,19]. So, multiplets are observed around at 9.14–7.38 ppm in **2**, **3**, **4** and **5** complexes and have been assigned to the aromatic protons of **2**, **3**, **4** and **5** metal complexes.

3.2. IR spectra

The infrared spectra of **1**, **2**, **3**, **4** and **5** metal complexes have been studied order to characterize their structures. The IR spectra of all metal chelates were carried out in the 4000–400 cm^{-1} range. The characteristic infrared spectrum data are given in Section 2. The υ(C=N) stretching vibrations are affected upon complexation and are situated at a frequency significantly different than the free ligand that the υ(C=N) peak observed at 1636 cm^{-1} for ligand. Coordination of the *vic*-dioxime ligands to the metal center
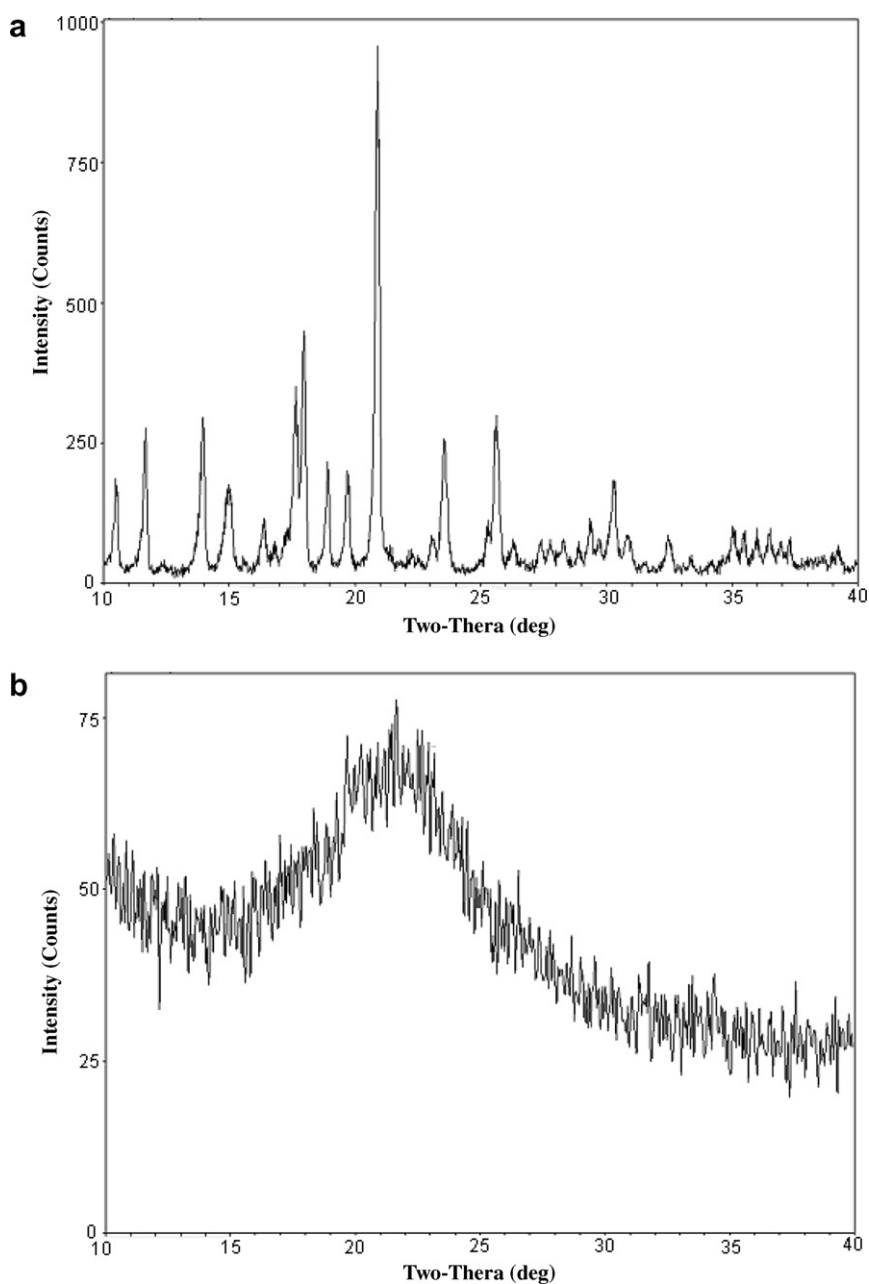
Fig. 3. X-ray powder diffractograms of (a) **1** and (b) **2** complexes.

through the four nitrogen atom are expected to reduce the electron density in the azomethine link and lower the $\upsilon(C=N)$ absorption frequency. The peak due to $\upsilon(C=N)$ are shifted to lower frequencies and appears between 1616 and 1597 cm^{-1}, indicating coordination of the azomethine nitrogen to the Pd metal [20]. However, the disappearance of $\upsilon(O-H)$ stretching bands in the IR spectrum of free ligand together with the existence of H-bridge (O−H··O) at 1692 cm^{-1} and the shifting of −C=N and −N−O strectches in the IR spectra of the **1** metal complexes provide support for MN$_4$-type coordinations in the metal complexes [21]. In the IR spectra of **2, 3, 4** and **5** metal complexes, the intramolecular hydrogen band was not observed, as expected. This is because the H-bonded (O−H··O) of mononuclear palladium complex disappeared upon an encapsulation of the ruthenium ions on the formation of trinuclear metal complexes, namely Ru$_2$(bpy)$_4$, Ru$_2$(phen)$_4$, Ru$_2$(dafo)$_4$, and Ru$_2$(dcbpy)$_4$. The spectra show strong peak at 1734 cm^{-1} for **4** and 1718 cm^{-1} for **5** due to carbonyl and carboxylic acid group. Perchlorate salts show strong antisymmetric stretching band at between 1088 and 1071 cm^{-1} and sharp antisymmetric stretching band at between 624 and 623 cm^{-1}, an indication of uncoordinated perchlorate anions [22]. The coordination of the bipyridine or phenantroline nitrogen is further supported by the appearance of a peak at 526–520 cm^{-1}, due to $\upsilon(Ru-N)$ stretching vibrations that are not observed in the infrared spectra of the ligand (LH)$_2$.

3.3. UV–VIS spectra

Electronic spectra of **1, 2, 3, 4** and **5** metal complexes have been recorded in the 1100–200 nm range in Acetone and DMF solutions and their corresponding data are given in Section 2. The UV–VIS spectra of the five metal complexes in Acetone showed 4–5 absorption bands between 277 and 567 nm and in DMF showed three-six absorption bands between 266 and 597 nm, respectively. In the electronic spectra of the five metal complexes, the wide a range bands seems to be due to both the $\pi \rightarrow \pi^*$, and $n \rightarrow \pi^*$ transitions of C=N and charge-transfer transition arising from π electron interactions between the metal and ligand which involves either a metal-to-ligand or ligand-to-metal electron transfer [23,24]. The absorption bands below 303 nm in Acetone or DMF are practically identical and can be attributed to $\pi \rightarrow \pi^*$ transitions in the benzene ring or azomethine (−C=N) groups. Azomethine groups are a useful tool for the fabrication of the new Pd^{II} and Ru^{II}–Pd^{II}–Ru^{II} metal complexes with specific electronic and structural properties. The absorption bands observed within the range of 309–351 nm in Acetone and the range of 311–395 nm in DMF are most probably due to the transition of $n \rightarrow \pi^*$ of imine group corresponding to the ligand or metal complexes [25]. For mononuclear **1** metal complexes, the absorption bands at range 432–434 nm are assigned to M $\rightarrow$ L charge transfer (MLCT) or L $\rightarrow$ M charge transfer (LMCT) [26], respectively. On complex formation, the electronic spectra of the **1** metal complexes exhibited significantly different absorption bands compared to those of the ligand in Acetone and DMF solutions. As expected, the new bands at range 432–434 nm arising from M $\rightarrow$ L charge transfer (MLCT) or L $\rightarrow$ M charge transfer (LMCT) transitions were observed as a result of coordination of palladium metal through azomethine nitrogen. These absorption bands are typical for mononuclear **1** metal complex with a square-planar structure. The complexes **2, 3, 4** and **5** exhibit a shoulder band around 420 with 567 nm and 450 with 597 nm in Acetone and DMF respectively, with the absorptivity of the former being higher. These spectra are similar to the other bpy, phen, dafo or dcbpy analogues and are assigned to the dπ(Ru^{II}) $\rightarrow$ π^* (bpy, phen, dafo or dcbpy) metal-to-ligand charge transfer (MLCT) transition. Examples of UV–VIS spectra of the ligand and their metal complexes were presented in Section 2.

3.4. Solubility and molar conductivity

The ligand is soluble in common organic solvents such as THF, C$_2$H$_5$OH, CH$_2$Cl$_2$, and DMSO. Although **1** are soluble in DMSO and DMF and slightly soluble in CH$_2$Cl$_2$, CHCl$_3$, trinuclear metal complexes **2, 3, 4** and **5** are highly soluble than **1** complex, due to the presence of Ru(bpy)$_2$, Ru(phen)$_2$, Ru(dafo)$_2$ or Ru(dcbpy)$_2$ bridged groups in the oxime moities. With a view to studying the electrolytic nature of the metal complexes, their molar conductivities were measured in DMF at 10^{-3} M. The molar conductivity (Λ_M) values of **1** metal complex is 33 Ω^{-1}cm^2 mol^{-1} at room temperature [27], indicating their almost non-electrolytic nature. Due to not free ions in **1** complex, the results indicate that this metal complex is very poor in molar conductivity. The molar conductivities (Λ_M) values of these trinuclear **2, 3, 4** and **5** metal complexes are range 208–211 Ω^{-1}cm^2 mol^{-1} at room temperature, indicating 1:2 electrolytes or three ionic species in solution [28].

3.5. Crystallography

Fig. 3 shows the X-ray powder diffraction data. For more clarity, a small window, representative of the whole range, restricted to the $10° < 2\theta < 40°$ is presented for the ligand and all metal complexes. We have attempted to prepare single crystals of ligand (LH$_2$) and **1, 2, 3, 4** and **5** metal complexes in different solvents, but we could not prepare convenient single crystals of ligand and
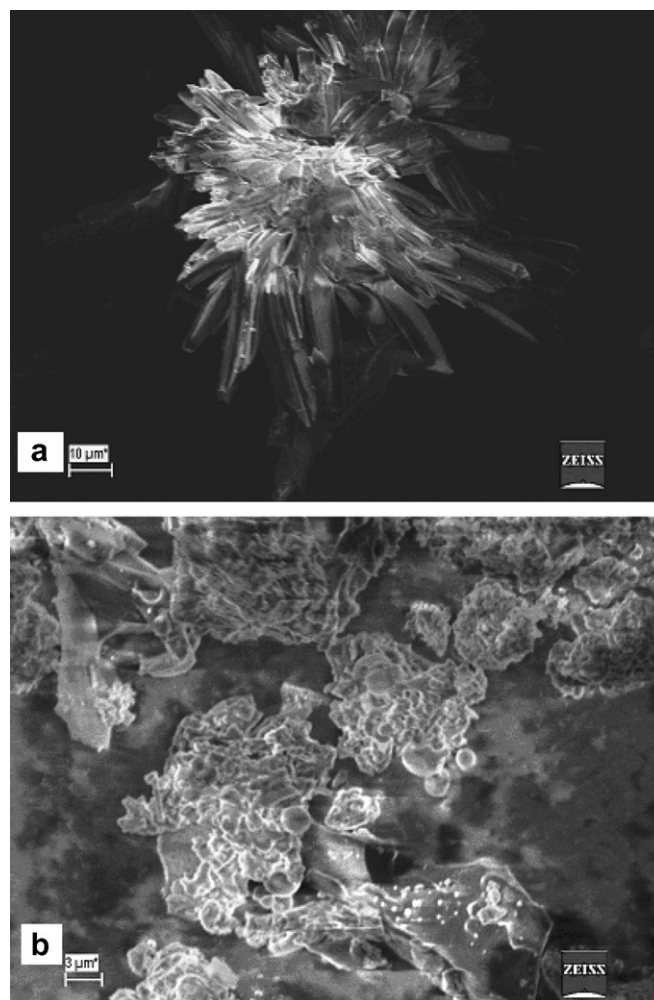

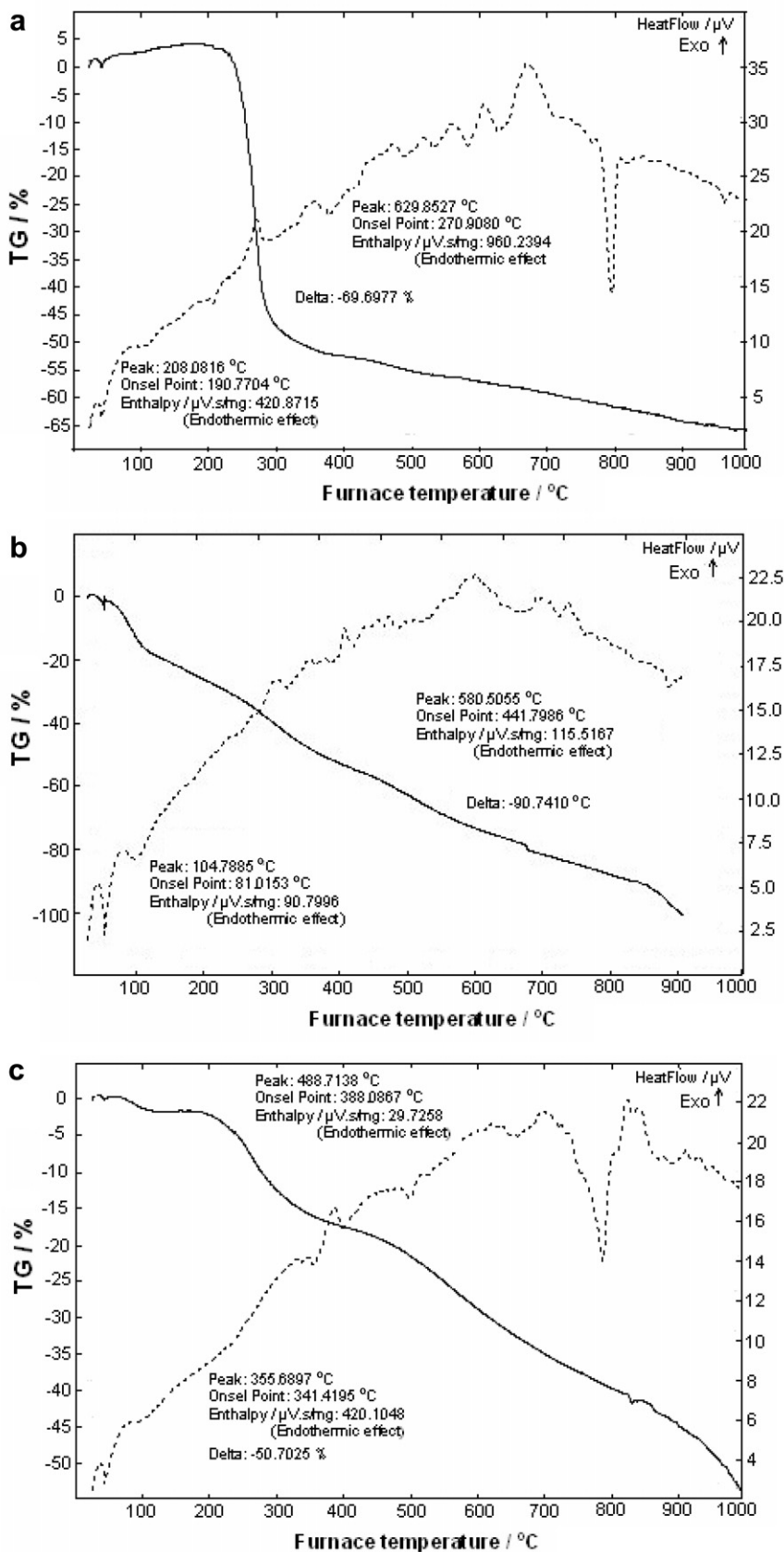**Fig. 4.** The SEM images of (a) **1** and (b) **4** metal complexes.

Fig. 5. The TGA and DTA curves of (a) **1**, (b) **4** and (c) **5** metal complexes.

all metal complexes. However, the crystalline nature of **1** complex and the amorphous nature **2**, **3, 4** and **5** metal complexes can be readily evidenced from their X-ray powder patterns. The **1** metal complex exhibit sharp reflections and all diffractograms are nearly

identical, indicating the isostructural nature of this compound. Also, the large number of reflections as well as their positions indicates a low crystal symmetry [23b,29]. This results show that **1** metal complex is indicating crystalline nature, not amorphous nature. Whereas, the X-ray powder pattern of the ligand (LH$_2$) with **2**, **3**, **4** and **5** exhibited only broad humps, indicating its amorphous nature.

3.6. Thermal properties

The thermal properties of the **1**, **4** and **5** metal complexes were investigated by thermal gravimetric analyses (TGA) and thermal differential analyses (DTA). Fig. 5a,b and c shows the recorded TGA and DTA curves of **1**, **4** and **5** metal complexes under a nitrogen atmosphere. The samples were heated up at 1 atm pressure with a heating rate of 10 °C min^{-1} a temperature range of 20–1000 °C. It can be seen that TGA curve of the **1** complex show no mass loss up to 177 °C (Fig. 5a), indicating the absence of water molecules and any other adsorptive solvents molecules in coordinate sphere. As the temperature is increased, the first decomposition stage occurred in the range 177–327 °C which is assigned to loss of C$_{24}$H$_{36}$N$_2$O$_4$ (organic rest) with a weight loss 51.2% and calculated value is 51.5%, the second decomposition stage occurred in the range 327–693 °C which is assigned to loss of C$_{12}$H$_{10}$ (organic moiety) with a weight loss 69.8% and calculated value is 70.5% (Fig. 5a). The thermal decomposition of **4** complex occurs at four steps and **5** complex occurs at three steps. The first degradation step take place in the range of 55–139 °C which is a weight loss 19% for **4** complex and in the range of 60–119 °C which is a weight loss 1.72% for **5** complex, the second degradation step take place in the range of 139–364 °C which is a weight loss 46% for **4** complex and in the range of 119–367 °C which is a weight loss 16.42% for **5** complex, the third degradation step take place in the range of 364–608 °C which is a weight loss 69% for **4** complex and in the range of 471–827 °C which is a weight loss 16.4% for **5** complex, the fourth degradation step take place in the range of 608–912 °C which is a weight loss 91% for **4** complex, respectively (Fig. 5b and c).

3.7. Catalytic tests

Among palladium-catalyzed cross-coupling processes, the Suzuki reaction of aryl/vinyl halides with boronic acid is one of the most efficient methods for C–C bond formation. Following optimization experiments we found that the reaction performed in mixture of DMF and water, with Cs$_2$CO$_3$ as the base at 90 °C appeared to be best. We initially tested the catalytic activity of the complexes **1**, **4** and **5** for the coupling of *p*-bromoacetophenone with phenylboronic acid and the control experiments showed that the coupling reaction did not occur in the absence of the catalyst. Under these conditions, *p*-bromoacetophenone and *p*-bromobenzaldehyde react cleanly with phenylboronic acid in good yields (Table 1). The palladium-catalyzed reaction of aryl halides with arylboronic acids (the Suzuki coupling reaction) is the most common method for C–C bond formation [30]. The reactions are usually carried out homogeneously in the presence of a base under inert atmosphere. The reactivity of the aryl halide component decreases sharply in the order X = I > Br > Cl and electron withdrawing substituents R are required for the chlorides to react [30,31]. The palladium-catalyzed cross-coupling reaction of phenylboronic acid with aryl bromides has been summarized in Table 1. As a base, Cs$_2$CO$_3$ [32] was the best choice and as a solvent mixture DMF (1.5 ml) and H$_2$O (1.5 ml) was found to be better than other solvents. From the results shown in Table 1, it is evident that the **1** complex is more efficient than the other complexes and has the more selectivity for this coupling reaction. The presence of the ruthenium metal in the **4** and **5** metal complexes have no signifi-

Table 1
The Suzuki coupling reaction of arylbromides with phenylboronic acid

Entry	R	Cat. (Complex)	Time (h)	Conversion (%)	Yield (%)[a]
1	CHO	**4**	1	59.2	58.5
2	CH$_3$CO	**4**	1	21.2	18.9
3	CHO	**1**	1	99.2	97.9
4	CH$_3$CO	**1**	1	98.1	97.6
5	CHO	**5**	1	23.3	21.2
6	CH$_3$CO	**5**	1	24.9	23.7
7	CHO	**4**	3	79.9	79.7
8	CH$_3$CO	**4**	3	34.8	33.9
9	CHO	**1**	3	99.5	99.3
10	CH$_3$CO	**1**	3	99.4	97.8
11	CHO	**5**	3	69.2	68.4
12	CH$_3$CO	**5**	3	32.2	31.6

Reaction conditions: 1.0 mmol of aryl bromide; 1.5 mmol of phenylboronic acid; 2.0 mmol Cs$_2$CO$_3$; 1.5% Pd (Cat.) was used; DMF 1.5 ml/H$_2$O 1.5 ml; Temperature 90 °C.
[a] GC-yield using diethyleneglycol-di-*n*-butylether as internal standard.

cant contribution the Suzuki coupling of the arly bromides. In addition the C=O bond in the **4** complex and the CO$_2$H grup in the **5** complex might be a negative effect on their catalytic activities.

4. Conclusions

In this study, the new *vic*-dioxime ligand and their mononuclear **1**, trinuclear **2**, **3**, **4** and **5** metal complexes were synthesized and characterized by elemental analyses, FT-IR, UV–VIS, ^{1}H NMR spectra, magnetic susceptibility measurements, molar conductivity, X-ray powder techniques and their morphology studied by SEM measurements. Although *vic*-dioximes complexes have been synthesized for a very long period of time, a few examples of their heteropolynuclear complexes have studied. This study presents a series of the mononuclear **1** and the trinuclear *vic*-dioxime complexes **2**, **3**, **4** and **5**, which were prepared by the coordination of Ru(bpy)$_2$, Ru(phen)$_2$, Ru(dafo)$_2$ or Ru(dcbpy)$_2$ bridged groups into the main palladium oxime moities. In the other studies, it is well known that the biological activities of Pd^{II}, Ph$_2$B–Pd^{II}–BPh$_2$ and Ru^{II}–Pd^{II}–Ru^{II} type metal complexes can be improved mixed-ligand complexes with heterocyclic bases, such as 1,10-phenanthroline, 2,2′-bipyridine, 4,4′-bipyridine, pyridine, 4,5-diazafluoren-9-one and 3,3′-dicarboxy-2,2′-bipyridine. The catalytic tests shown that **1** complex is an active catalyst in the coupling of 4-bromobenzaldehyde and 4-bromoacetophenone with phenylboronic acid. But **4** and **5** metal complexes appear to be less efficient as catalyst for the Suzuki coupling reactions. Also, the thermal results shown that the most stable complex is **1** compound while the less stable is compound **4**.

References

[1] B.Z. Shan, Q. Zhao, N. Goswami, D.M. Eichhorn, D.P. Rillema, Coord. Chem. Rev. 211 (2001) 117.
[2] M. Murali, M. Palaniandavar, Polyhedron 26 (14) (2007) 3980.
[3] F. Barigelletti, L. Flamigni, Chem. Soc. Rev. 29 (2000) 1.
[4] A. Erdem, K. Kerman, B. Meric, D. Ozkan, P. Kara, M. Ozsoz, Turk. J. Chem. 26 (2002) 851.
[5] C. Metcalfe, J.A. Thomas, Chem. Soc. Rev. 32 (2003) 215.
[6] (a) B.J. Coe, N.M.R. Curati, Comments Inorg. Chem. 25 (2004) 147;
(b) W.Z. Alsindi, T.L. Easun, X.Z. Sun, K.L. Ronayne, J.M. Herrera, M.W. George, M.D. Ward, Inorg. Chem. 46 (2007) 3696;
(c) P.J. Low, Dalton Trans. (2005) 2821.
[7] R.C. Evans, P. Dougles, C.J. Winscom, Coord. Chem. Rev. 250 (2006) 2093.

[8] (a) K. Ocakoglu, C. Zafer, B. Cetinkaya, S. Icli, Dyes Pigments 75 (2007) 385;
(b) T.J. Meyer, Pure Appl. Chem. 58 (1986) 193.
[9] (a) B.P. Sullivan, J.A. Baumann, T.J. Meyer, D.J. Salmon, H. Lehmann, A. Ludi, J. Am. Chem. Soc. 99 (1977) 7368;
(b) W.H. Fung, W.Y. Fu, C.M. Che, J. Org. Chem. 63 (1998) 7715;
(c) T.H. Ghaddar, E.W. Castner, S.S. Isied, J. Am. Chem. Soc. 122 (2000) 1233.
[10] (a) E. Bell-Loncella, C.A. Bessel, Inorg. Chim. Acta 303 (2000) 199;
(b) A. Kilic, I. Yilmaz, M. Ulusoy, E. Tas, Appl. Organometal. Chem. (in press).
[11] R. Llanguri, J.J. Morris, W.C. Stanley, E.T. Bell-Loncella, M. Turner, W.J. Bayko, C.A. Bessel, Inorg. Chim. Acta 315 (2001) 53.
[12] A. Earnshaw, Introduction to Magnetochemistry, Academic Press, London, 1968. p. 4.
[13] A. Kilic, E. Tas, B. Deveci, I. Yilmaz, Polyhedron 26 (2007) 4009.
[14] A. Kilic, E. Tas, B. Gumgum, I. Yilmaz, Polish J. Chem. 80 (2006) 1967.
[15] B.J. Sullivan, D.J. Salmon, T.J. Meyer, Inorg. Chem. 17 (1978) 3334.
[16] L.J. Hendersen, F.R. Fronczek, W.R. Cherry, J. Am. Chem. Soc. 106 (1984) 5876.
[17] I.F. Eckhard, L.A. Summers, Aust. J. Chem. 26 (1973) 2727.
[18] P.J. Steel, E.C. Constable, J. Chem. Soc., Dalton Trans. (1990) 1389.
[19] (a) E. Bell-Loncella, C.A. Bessel, Inorg. Chim. Acta 303 (2000) 199;
(b) F.E. Lytle, L.M. Petrosky, L.R. Carlson, Anal. Chim. Acta 57 (1971) 239.
[20] (a) A. Kilic, E. Tas, B. Gumgum, I. Yilmaz, Chinese J. Chem. 24 (2006) 1599;
(b) S.A. Ali, A.A. Soliman, M.M. Aboaly, R.M. Ramadan, J. Coord. Chem. 55 (2002) 1161.
[21] (a) M. Kandaz, A. Koca, A.R. Özkaya, Polyhedron 23 (2004) 1987;
(b) E. Tas, M. Aslanoglu, A. Kilic, Z. Kara, J. Coord. Chem. 59 (8) (2006) 861.
[22] M.R. Rosenthall, T. Chem. Edu. 50 (1973) 331.
[23] (a) L. Sacconi, M. Ciampolini, F. Maffio, F.P. Cavasino, J. Am. Chem. Soc. 84 (1962) 3245;

[24] R.L. Carlin, Trans. Met. Chem., vol. 1, Marcel Dekker, New York, 1965.
[25] (a) C. Fraser, B. Bosnich, Inorg. Chem. 33 (1994) 338;
(b) S. Ilhan, H. Temel, I. Yilmaz, A. Kilic, Trans. Met. Chem. 32 (2007) 344.
[26] A.B.P. Lever, Inorganic Electronic Spectroscopy, Elsevier, Amsterdam, 1984.
[27] (a) R.L. Dutta, Inorganic Chemistry, Part II, 2nd ed. The New Book Stall, Calcutta, 1981, p. 386.;
(b) A. Kilic, E. Tas, B. Gumgum, I. Yilmaz, Heteroatom Chem. 18 (6) (2007) 657;
[c] M.S. Refat, S.A. El-Korashy, D.N. Kumar, A.S. Ahmad, Spectrochim. Acta. doi:10.1016/j.saa.2007.10.005.;
[d] M.S. Refat, J. Mol. Struct. 742 (1–3) (2007) 24.
[28] [a] W. Gary, J. Chem. Rev. 7 (1971) 81;
[b] B. Murphy, J. Nelson, S.M. Nelson, M.G.B. Drew, P.C. Yates, J. Chem. Soc., Dalton Trans. 123 (1987);
[c] D.S. Kumar, V. Alexander, Polyhedron 18 (1999) 1561.
[29] [a] B.R. Srinivasan, N.S. Dhuri, C. Nathar, W. Bensch, Trans. Met. Chem. 32 (2007) 64;
[b] B. Laik, M. Durandetti, J. Perichon, J. Electroanal. Chem. 602 (2007) 275.
[30] [a] N. Miyaura, A. Suzuki, Chem. Rev. 95 (1995) 2457;
[b] A.J. Suzuki, J. Organomet. Chem. 576 (1999) 147;
[c] S.P. Stanforth, Tetrahedron 54 (1998) 263;
[d] G.T. Crisp, Chem. Soc. Rev. 27 (1998) 427;
[e] N.J. Whitcombe, K.K. Hii, S.E. Gibson, Tetrahedron 57 (2001) 7449.
[31] [a] A.F. Littke, G.F. Fu, Angew. Chem., Int. Ed. Eng. 41 (2002) 4176;
[b] R.B. Bedford, S.L. Hazewood, M.E. Limmeat, Chem. Commun. (2002) 2610.
[32] C. Zhang, J. Huang, M.L. Trudell, S.P. Nolan, J. Org. Chem. 64 (1999) 3804.